Title
Let-7 and miR-125 cooperate to prime progenitors for astrogliogenesis

Journal
The EMBO Journal, 34(9)

ISSN
0261-4189

Authors
Shenoy, Archana
Danial, Muhammad
Blelloch, Robert H

Publication Date
2015-05-05

DOI
10.15252/embj.201489504

Peer reviewed

Article

SOURCE DATA | TRANSPARENT PROCESS

THE EMBO JOURNAL

Let-7 and miR-125 cooperate to prime progenitors for astrogliogenesis

Archana Shenoy, Muhammad Danial & Robert H Blelloch*

Abstract

The molecular basis of astrocyte differentiation and maturation is poorly understood. As microRNAs have important roles in cell fate transitions, we set out to study their function during the glial progenitor cell (GPC) to astrocyte transition. Inducible deletion of all canonical microRNAs in GPCs *in vitro* led to a block in the differentiation to astrocytes. In an unbiased screen, the reintroduction of let-7 and miR-125 families of microRNAs rescued differentiation. Let-7 and miR-125 shared many targets and functioned in parallel to JAK-STAT signaling, a known regulator of astrogliogenesis. While individual knockdown of shared targets did not rescue the differentiation phenotype in microRNA-deficient GPCs, overexpression of these targets in wild-type GPCs blocked differentiation. This finding supports the idea that microRNAs simultaneously suppress multiple mRNAs that inhibit differentiation. MicroRNA-regulated transcripts exhibited concordant changes during *in vivo* differentiation and were enriched for a gene set upregulated in glioblastomas, consistent with validity of using the *in vitro* model to study *in vivo* events. These findings provide insight into the microRNAs and the genes they regulate in this important cell fate transition.

Keywords astrocytes; differentiation; Let-7; microRNAs; miR-125
Subject Categories Neuroscience; RNA Biology
DOI 10.15252/embj.201489504 | Received 11 July 2014 | Revised 15 January 2015 | Accepted 16 January 2015 | Published online 23 February 2015
The EMBO Journal (2015) 34: 1180–1194

See also: **C Eitan & E Hornstein** (May 2015)

Introduction

Astrocytes are a dominant cell type in the central nervous system (CNS), intimately associated with neuronal synapses and CNS function (Zhang & Barres, 2010). They have come under renewed focus due to discoveries of their roles in driving evolutionary adaptations for central nervous system function and increased cognition in humans (Han *et al*, 2013; Xie *et al*, 2013). While the number of studies examining mature astrocyte function is growing, very little is known about the molecular mechanisms underlying their specification and differentiation from glial precursors during development.

During embryogenesis, neuroepithelial stem cells give rise to radial glial cells, which are initially restricted to a neurogenic fate. Near the end of embryogenesis and in early postnatal stages, the progeny of many of these cells become restricted to a glial progenitor fate and give rise to astrocytes and oligodendrocytes (Rowitch & Kriegstein, 2010). The switch from neurogenesis to astrogliogenesis is mediated by a number of mechanisms including activation of JAK-STAT signaling and silencing of the neurogenic bHLH factors. Recent studies have also identified the transcription factors Sox9 and NF1A/B as being instructive for astrogliogenesis (Molofsky *et al*, 2012). *In vitro*, embryonic stem cells (ESCs) can be induced to follow the same sequential steps as seen *in vivo* providing a powerful tool to dissect the transcriptional and post-transcriptional events underlying each step in astrocyte differentiation (Okabe *et al*, 1996; Brüstle & McKay, 1999; Krencik *et al*, 2011).

MicroRNAs (miRNAs) play a major role in post-transcriptional regulation. They are small non-coding RNAs that destabilize and inhibit translation of their target mRNAs (Krol *et al*, 2010). Once transcribed, canonical miRNAs are processed by a complex composed of the RNA binding protein Dgcr8 and RNaseIII enzyme Drosha, into hairpin structures called pre-miRNAs. They are then exported to the cytoplasm and further processed by the enzyme Dicer into 18–21 nucleotide duplexes, one strand of which is loaded into a silencing complex consisting of Argonaute proteins. Once loaded into the silencing complex, miRNAs bind targets through partial base pairing with mRNAs through a 6–8 nucleotide seed sequence at the 5′ end of the miRNA. This minimal base-pairing requirement enables a single miRNA to target hundreds of mRNAs. Additionally, miRNA targets form networks of genes that collaborate to promote or inhibit cell fate transitions (Judson *et al*, 2013). Therefore, identifying the major miRNAs and their downstream target gene network can provide novel insight into cell fate transitions.

In the neural lineage, detailed information on the function of miRNAs has been mostly limited to neuronal and oligodendrocyte differentiation (Krichevsky *et al*, 2009; Zhao *et al*, 2009, 2010b; Dugas *et al*, 2010). For example, it has been shown that distinct sets of miRNAs, miR-9/124 in neurons and miR-219/338 in oligodendrocytes, are highly upregulated during differentiation of progenitors and that these miRNAs play key roles in driving differentiation by

Eli and Edythe Broad Center of Regeneration Medicine and Stem Cell Research, Center for Reproductive Sciences and Department of Urology, University of California San Francisco, San Francisco, CA, USA
*Corresponding author. Tel: +1 415 476 2838; E-mail: blellochr@stemcell.ucsf.edu

inhibiting mRNAs that maintain the progenitor state. Two studies have suggested that miRNAs are required for production of astrocytes by deleting Dicer in spinal cord progenitors and in *in vivo* derived multipotent neural stem cells (Andersson *et al*, 2010; Zheng *et al*, 2010b). However, further characterization in these experimental settings is complicated by the inability to isolate large numbers of astrocyte progenitors. In particular, *in vivo* astrocyte progenitors are transient, non-uniform in their spatial and temporal differentiation, and so far lack distinct markers to allow purification (Freeman, 2010).

In this study, we sought to overcome this roadblock by using an established *in vitro* counterpart to *in vivo* astrocyte differentiation (Brüstle & McKay, 1999). The *in vitro* method leads to the production of homogenous populations of glial progenitor cells (GPCs) that can be induced to differentiate in synchrony into astrocytes under defined culture conditions. Here, we characterize a differentiation phenotype associated with the loss of Dgcr8 and identify miRNAs and their target genes that in part underlie this phenotype. Additionally, we show that the miRNA targets are modulated during *in vivo* astrocyte development and during glioma progression. These studies provide a detailed characterization of how miRNAs promote the GPC to astrocyte transition, a critical aspect of the development of a functional nervous system.

Results

Development of *in vitro* astrocyte differentiation system for the study of miRNA function

To study the role of microRNAs in glia progenitor cells, we took advantage of a conditional knockout model for *Dgcr8*, which encodes an essential cofactor in the biogenesis of all canonical miRNAs (Wang *et al*, 2007). An *in vitro* model was critical for evaluating miRNA function as astrocyte progenitors cannot be isolated in large numbers or as a homogenous population from *in vivo* tissue. Thus, a ubiquitously expressed tamoxifen-inducible Cre recombinase was targeted into the Rosa26 locus in mouse embryonic stem cells (ESCs) that were hemizygous for the exon 3 floxed allele of Dgcr8 (*R26 CreER*; $Dgcr8^{flox/\Delta}$) (Supplementary Fig S1A). The floxed ESCs, which produce Dgcr8 and microRNAs at wild-type levels, were differentiated into glial progenitor cells (GPCs) using an established neural differentiation protocol (Okabe *et al*, 1996; Brüstle & McKay, 1999; Wang *et al*, 2007) (Supplementary Fig S1B). The resulting neural progenitors were initially largely restricted to a neurogenic fate. With continued passaging in the presence of FGF and EGF, they lost neurogenic potential and became restricted to a glial progenitor fate (GPCs). Withdrawal of growth factors along with addition of either serum or BMP-4 led to an almost exclusive differentiation to $GFAP^+$ astrocyte-like cells (Supplementary Fig S1C).

Microarray data on the *in vitro* derived GPCs and differentiated astrocytes were compared to previously published transcriptome data for *in vivo* purified mature astrocytes, oligodendrocytes and neurons (Lovatt *et al*, 2007; Cahoy *et al*, 2008). The *in vitro* derived cells expressed a majority of genes previously found to be enriched within *in vivo* purified astrocytes, and to a much lesser degree those expressed in oligodendrocytes and neurons (Supplementary Fig S1D). Many of these genes were expressed in both the GPC and astrocyte populations, although a number of genes further upregulated in the astrocytes, such as Aqp4 (Supplementary Fig S1E), a gene essential for mature *in vivo* astrocyte function (Xie *et al*, 2013). The absence of expression of some astrocyte genes *in vitro* likely reflects incomplete maturation, a common feature of adult cell types derived from ESCs *in vitro* (Nicholas *et al*, 2013). Importantly, transplantation of the glial progenitors gave rise to cells that had astrocyte morphology and expressed GFAP when assessed 6 weeks after injection (Supplementary Fig S1F). These results confirm that the *in vitro* model recapitulates many aspects of *in vivo* astrocyte differentiation.

Dgcr8 loss in ESC-derived GPCs leads to separable differentiation and survival defects

To study the effect of conditional loss of miRNAs during the GPC to astrocyte transition, all experiments were done with *R26 CreER;* $Dgcr8^{flox/\Delta}$ GPCs plus/minus tamoxifen after 6–10 passages in bFGF and EGF. Tamoxifen treatment of GPCs for 24–48 h led to 100-fold reduction of Dgcr8 and approximately 50-fold reduction of highly expressed miRNAs at 5–7 days post-treatment consistent with efficient and stable loss of Dgcr8 in the majority of the cell population (Fig 1A and B).

As miRNA knockout GPCs ($Dgcr8^{\Delta/\Delta}$) survived and continued to proliferate, we investigated the global requirement for miRNAs in serum-induced differentiation of GPCs to astrocytes. The $Dgcr8^{\Delta/\Delta}$ GPCs showed a striking inability to upregulate GFAP (Fig 1C). In contrast, untreated $Dgcr8^{flox/\Delta}$ cells and *R26 CreER* cells treated with tamoxifen (both serving as controls) differentiated normally. The small number of $Dgcr8^{\Delta/\Delta}$ cells that do differentiate likely represents cells that failed to excise exon 3 of the second allele of *Dgcr8*. During differentiation of $Dgcr8^{\Delta/\Delta}$ GPCs, we observed an increase in apoptosis at 8–10 h post-differentiation, as quantified by flow cytometry using Annexin V and a vital dye (Supplementary Fig S2A). Consistent with the increase in Annexin V-positive cells, Western blot analysis showed an increase in the apoptotic marker cleaved caspase-3 (Fig 1D). Together, these results uncover an essential role for Dgcr8 in astrocyte differentiation and a partially penetrant role in cell survival.

The reduced survival raised the possibility that the differentiation defect in $Dgcr8^{\Delta/\Delta}$ GPCs may be secondary to apoptosis. To address this possibility, we took advantage of an apoptosis-resistant *Dgcr8* conditional model (Wang *et al*, 2013). *R26 CreER*; $Bak^{\Delta/\Delta}$; $Bax^{f/\Delta}$; $Dgcr8^{f/\Delta}$ ESC-derived GPCs were used, in which tamoxifen treatment led to a simultaneous loss of Bax and Dgcr8 (referred to as triple knockout TKO) and a complete absence of apoptosis during differentiation (Supplementary Fig S2B and C). Despite a lack of observable cell death, the knockout cells continued to show a striking defect in differentiation (Fig 1E). In contrast, untreated cells or tamoxifen-treated cells carrying $Dgcr8^{+/+}$ in the $Bax^{f/f}$;$Bak^{\Delta/\Delta}$ background differentiated normally (Fig 1E), consistent with previously published findings (Lindsten *et al*, 2003). Of note, the removal of *Bax* and *Bak* led to increased cell number in wild-type as well as *Dgcr8* knockout cells, showing that appreciable apoptosis occurs in the wild-type context as well, although to a lesser degree than in the *Dgcr8* knockout cells. Together, these data show that Dgcr8 is essential for GPC differentiation independent of its suppression of apoptosis.

Finally, we asked whether the defect in differentiation was associated with defective upregulation of astrocyte genes. Therefore, we

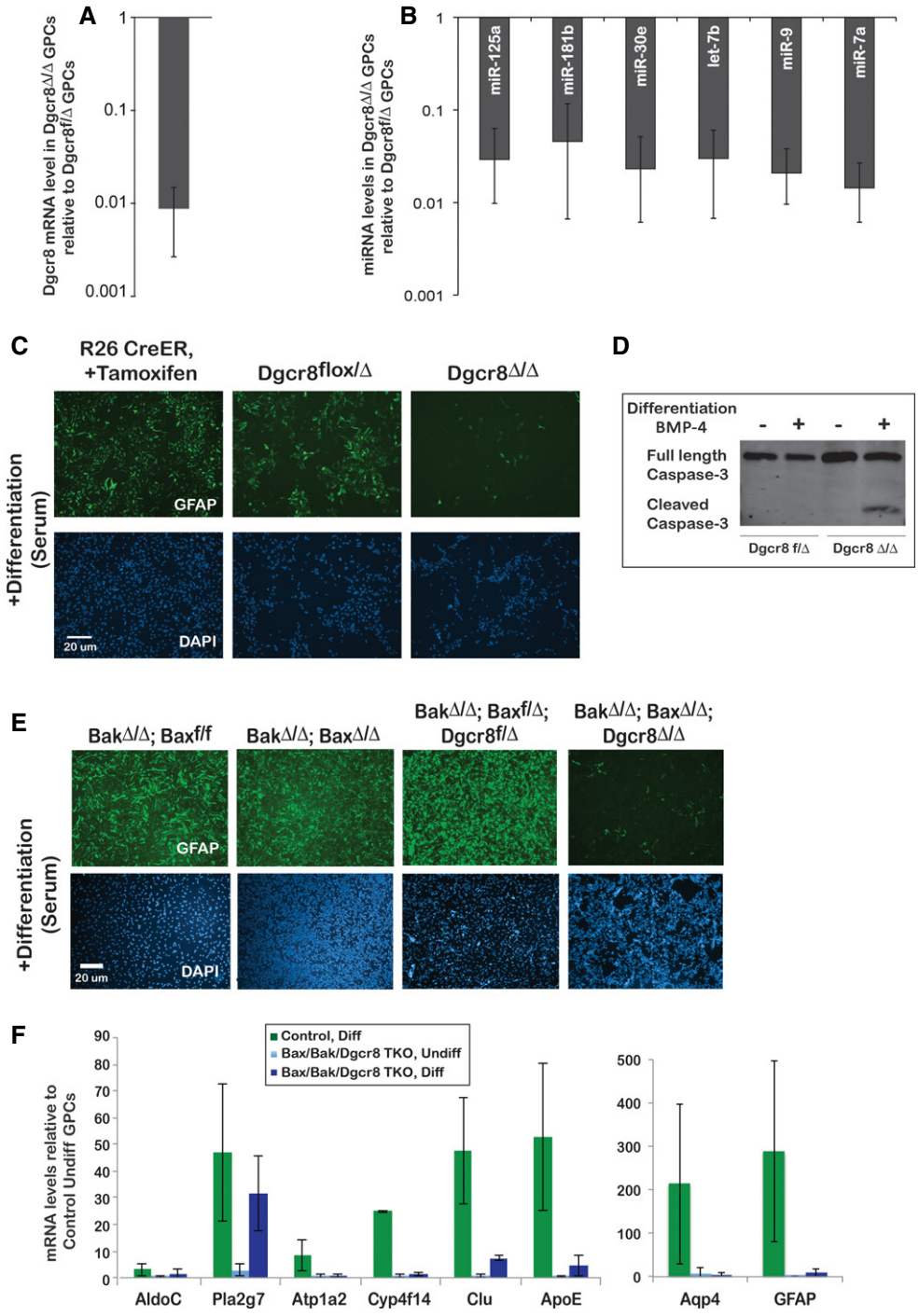

Figure 1. Dgcr8 loss leads to separable differentiation and survival defects in GPCs.

A RT–qPCR of Dgcr8 exon 3 in *Dgcr8*$^{\Delta/\Delta}$ GPCs 5–7 days following tamoxifen treatment (n = 3). Samples were normalized to actin, and data are presented relative to untreated *Dgcr8*$^{flox/\Delta}$ GPCs.

B RT–qPCR for a panel of miRNAs in *Dgcr8*$^{\Delta/\Delta}$ cells 5–7 days post-tamoxifen treatment (n = 3). Samples are normalized to U6 RNA.

C Representative images of GFAP immunofluorescence following 48 h of differentiation in control (*R26 CreER* + tamoxifen and untreated *Dgcr8*$^{flox/\Delta}$ GPCs) and *Dgcr8*$^{\Delta/\Delta}$ GPCs.

D Representative Western blot of full length and cleaved caspase-3 levels in control and *Dgcr8*$^{\Delta/\Delta}$ cells following 5–6 hours of differentiation (n = 2).

E Representative images of GFAP immunofluorescence following 48 h of differentiation in *Bak*$^{\Delta/\Delta}$;*Bax*$^{f/f}$ (control), *Bak*$^{\Delta/\Delta}$;*Bax*$^{\Delta/\Delta}$ (control), *Bak*$^{\Delta/\Delta}$;*Bax*$^{flox/\Delta}$;*Dgcr8*$^{flox/\Delta}$ GPCs (control) and *Bak*$^{\Delta/\Delta}$;*Bax*$^{\Delta/\Delta}$;*Dgcr8*$^{\Delta/\Delta}$ (TKO) cells (n = 3).

F RT-qPCR for panel of astrocyte markers in control and *Bak*$^{\Delta/\Delta}$;*Bax*$^{\Delta/\Delta}$;*Dgcr8*$^{\Delta/\Delta}$ cells (n = 3).

Data information: In all panels, error bars represent SD. Scale bars as shown.
Source data are available online for this figure.

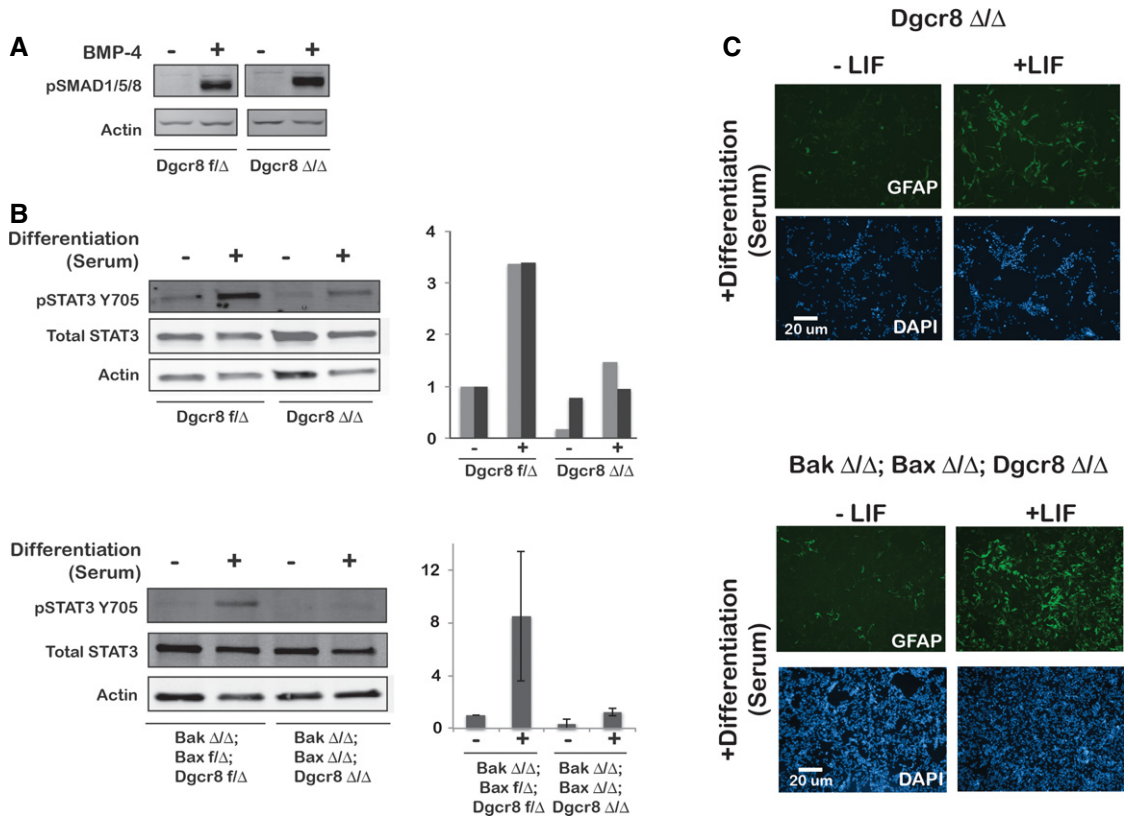

Figure 2. Rescue of JAK-STAT signaling leads to partial rescue of differentiation defect in GPCs.

A Western blot assaying level of pSMAD 5–6 h following BMP-4 addition in control and *Dgcr8*$^{\Delta/\Delta}$ cells (n = 2).

B Western blots and quantification (right panels, relative to actin) showing levels of pSTAT3 Y705 and total STAT3. Upper panel: Data for *Dgcr8*$^{flox/\Delta}$ (control) and *Dgcr8*$^{\Delta/\Delta}$ cells 5–6 h following serum differentiation (n = 2). Light grey and dark grey bars represent the data for 2 experiments. Lower panel: Data for *Bak*$^{\Delta/\Delta}$;*Bax*$^{flox/\Delta}$; *Dgcr8*$^{flox/\Delta}$ GPCs (control) and *Bak*$^{\Delta/\Delta}$;*Bax*$^{\Delta/\Delta}$;*Dgcr8*$^{\Delta/\Delta}$ (TKO) cells during serum differentiation (n = 3). Quantification is shown on the right; error bars represent standard deviation.

C Representative images of GFAP immunofluorescence of *Dgcr8*$^{\Delta/\Delta}$ and *Bak*$^{\Delta/\Delta}$;*Bax*$^{\Delta/\Delta}$;*Dgcr8*$^{\Delta/\Delta}$ cells and respective controls following 48 h of differentiation in the presence or absence of LIF (n = 3). Scale bars as shown.

Source data are available online for this figure.

performed RT-qPCR on a panel of markers enriched in astrocytes during differentiation of TKO and control cells. The astrocyte markers Aqp4, ApoE, Clu, Atp1a2 and Cyp4f14 failed to be upregulated in the TKO in stark contrast to control cells (Fig 1F). However, AldoC and Pla2g7 were upregulated similar to control cells. Therefore, Dgcr8 is required for the upregulation of many, but not all, genes associated with astrocyte differentiation.

Induction of JAK-STAT pathway rescues *Dgcr8*$^{\Delta/\Delta}$ differentiation defect

Normal astrogliogenesis requires activation of BMP signaling and JAK-STAT signaling (Bonni *et al*, 1997; Fan *et al*, 2005; He *et al*, 2005). For a number of astrocyte genes such as GFAP, phosphorylated STAT3 forms a complex with SMAD and p300 and binds to their promoter to activate transcription (Fukuda *et al*, 2007). In cultures of *in vivo* derived cortical neural stem cells, phosphorylation of STAT3 at tyrosine 705 increases coincident with astrocyte differentiation of cortical neural stem cells and inhibition of STAT3 abrogates astrocyte differentiation.

To determine whether BMP or JAK-STAT signaling is disrupted upon miRNA loss, we examined the downstream mediators of the two pathways, phosphorylated SMAD and STAT3 (pSMAD and pSTAT3), in control and *Dgcr8*$^{\Delta/\Delta}$ GPCs during differentiation. The addition of BMP-4 robustly activated pSMAD in control *Dgcr8*$^{f/\Delta}$ GPCs. The activation of pSMAD was unaffected in *Dgcr8*$^{\Delta/\Delta}$ GPCs under the same conditions (Fig 2A). In contrast to pSMAD, pSTAT3 was significantly reduced in *Dgcr8*$^{\Delta/\Delta}$ cells during both basal growth and differentiation conditions (Fig 2B and Supplementary Fig S3A). Approximately 6–12 h following the shift to differentiation conditions, pSTAT3 in *Dgcr8*$^{\Delta/\Delta}$ cells showed an increase in levels but still only reaching basal levels of *Dgcr8*$^{f/\Delta}$ GPCs. *Dgcr8*$^{f/\Delta}$ showed a three- to fourfold increase under the same conditions. Total STAT3 levels were unchanged. Similar results were seen in the Bak/Bax/Dgcr8 TKO background showing that this defect in STAT3 phosphorylation occurs independently of apoptosis (Fig 2B).

To further test the role of STAT3 signaling in the differentiation defect, we introduced activators and inhibitors of the pathway. First, to confirm that JAK-STAT signaling was necessary for astrocyte differentiation in ESC-derived GPCs, a small molecule inhibitor

targeting JAK (JAKi) was added during differentiation of wild-type cells. JAK inhibition abrogated the expression of GFAP during differentiation (Supplementary Fig S3B). Next, to activate the JAK-STAT pathway in *Dgcr8*$^{\Delta/\Delta}$ cells, leukemia inhibitory factor (LIF), a canonical activator, was introduced along with FBS to increase STAT3 phosphorylation (Supplementary Fig S3C). Addition of LIF led to a consistent increase in the number of GFAP-positive cells in both *Dgcr8*$^{\Delta/\Delta}$ and TKO backgrounds (Fig 2C). Together, these data suggest that a decrease in JAK-STAT signaling is at least partially responsible for the defect in astrocyte differentiation seen upon *Dgcr8* loss.

Let-7 and miR-125 families of miRNAs are highly expressed in GPCs and rescue the *Dgcr8*$^{\Delta/\Delta}$ differentiation defect

As the predominant role of Dgcr8 is in miRNA biogenesis (Preiss, 2009; Barad *et al*, 2012; Seong *et al*, 2014), we next sought to identify specific miRNAs that may underlie the differentiation defect of *Dgcr8*$^{\Delta/\Delta}$ cells by simultaneously profiling and functionally screening miRNAs. In a number of lineages, miRNAs that promote differentiation increase upon induction of differentiation and promote downregulation of the progenitor transcriptional program (Yoo *et al*, 2009; Dugas *et al*, 2010; Goljanek-Whysall *et al*, 2011). Therefore, we performed small RNA sequencing of GPCs in proliferation conditions and following 48 h of serum differentiation. Surprisingly, levels of the most abundant miRNAs were largely unchanged following 48 h of differentiation, even though the cells express GFAP and other markers of differentiated astrocytes as well as develop characteristic astrocyte morphology by this time point (Fig 3A, Supplementary Figs S1E and S4). This finding suggested that miRNAs already expressed in the proliferating progenitors are required for the production of astrocytes.

To uncover the impact of miRNA loss on the transcriptome of GPCs, we profiled mRNAs in *Dgcr8*$^{\Delta/\Delta}$ versus control *Dgcr8*$^{f/\Delta}$ GPCs in proliferation conditions. As has been previously shown in other cell types, the global loss of miRNAs led to hundreds of misregulated mRNAs (Fig 3B) (Sinkkonen *et al*, 2008; Yi *et al*, 2009; Gurtan *et al*, 2013). To determine whether these mRNAs represent targets of expressed miRNAs, the downregulated and upregulated gene sets were evaluated for enriched 7-mer motifs in an unbiased fashion. Among upregulated genes, 104 enriched motifs were uncovered ($P < 0.01$). Many of the most highly enriched motifs perfectly matched the seed region of four of the most highly expressed miRNA families including let-7, miR-9, miR-181 and miR-30, consistent with these miRNAs having a major effect on the GPC transcriptome ($P < 2.2e^{-16}$, Fig 3C, Supplementary Table S1). These data show that Dgcr8 loss leads to misregulation of many genes, a large fraction of which can be directly linked to expressed miRNAs.

Previous studies have shown that the addition of a single miRNA is sufficient to rescue individual phenotypes seen with global miRNA loss (Giraldez *et al*, 2005; Wang *et al*, 2008; Dugas *et al*, 2010; Melton *et al*, 2010; Zhao *et al*, 2010b; Steiner *et al*, 2011). We therefore performed a genome-wide screen for individual miRNAs that could rescue the capacity of the cells to differentiate to GFAP$^+$ cells. Specifically, 570 chemically synthesized miRNA mimics were added to individual wells of proliferating *Dgcr8*$^{\Delta/\Delta}$ GPCs, which were then transferred to differentiating conditions with serum (Fig 4A). Using the criteria outlined in Materials and Methods, we identified let-7 and miR-125 families of miRNAs as positive hits (Fig 4B). Validation experiments with independently synthesized mimics confirmed let-7 and miR-125 as positive hits, showing a striking rescue of GFAP expression in *Dgcr8*$^{\Delta/\Delta}$ GPCs in differentiation media (Fig 4C, Supplementary Fig S5E). The let-7 and miR-125 miRNA families have highly distinct seed sequences suggesting potential interdependent effects. Indeed, the simultaneous introduction of let-7 and miR-125 mimics led to a synergistic increase in the number of GFAP-positive *Dgcr8*$^{\Delta/\Delta}$ cells, suggesting that they cooperate to promote astrocyte differentiation (Fig 4D). Rescue of GFAP was also seen with introduction of let-7 and miR-125 into Bax/Bak/Dgcr8 TKO GPCs (Supplementary Fig S5A). Additional markers confirmed rescue of astrocyte differentiation following let-7 or miR-125 transfection including quantitative RT-qPCR for GFAP, Aqp4, Clu and ApoE (Fig 4E). However, there was no detectable increase in Atp1a2 and Cyp4f14. The lack of complete rescue of levels may reflect lower than complete transfection efficiency or partial rescue by the microRNAs. Levels of AldoC and Pla2g7 were up as seen even in the absence of miRNAs in Fig 1E. Importantly, cells transfected with let-7 and miR-125 did not upregulate markers of the oligodendrocyte (MBP) or neuronal (Tuj1) fate (Supplementary Fig S5B). Rescued cells also expressed the astrocyte marker vimentin (Supplementary Fig S5C). Together, these data show that let-7 and miR-125 rescue many aspects of astrocyte differentiation in otherwise miRNA- deficient cells.

Let-7 and miR-125 are highly expressed in both GPCs and astrocytes suggesting that they enable rather than induce astrocyte differentiation (Fig 3A). That is, they suppress mRNAs that encode proteins that when overexpressed in GPCs block differentiation. If true, these miRNAs should not be sufficient to induce differentiation. To test this directly, let-7 and miR-125 mimics were introduced into *Dgcr8*$^{\Delta/\Delta}$ GPCs that were maintained in proliferation conditions. Under these conditions, *Dgcr8*$^{\Delta/\Delta}$ GPCs remained undifferentiated (Supplementary Fig S5D), indicating that these miRNAs are not sufficient to induce differentiation. From these data, we conclude that let-7 and miR-125 repress targets in *Dgcr8*$^{\Delta/\Delta}$ GPCs that otherwise form a barrier to astrogliogenesis.

Identification and functional testing of mRNA targets of let-7 and miR-125

Next, we aimed to uncover the pathways and mRNAs regulated by these two miRNAs. Initially, we took a candidate approach and evaluated the JAK-STAT pathway based on our finding that the STAT3 signaling was reduced in *Dgcr8*$^{\Delta/\Delta}$ under both proliferation and differentiation culture conditions and that introduction of exogenous LIF could at least partially rescue differentiation (Fig 2). First, we asked whether the miRNAs could increase the levels of pSTAT3 in differentiation conditions, placing the miRNAs upstream of STAT3 phosphorylation (Fig 4F). However, the introduction of let-7 and miR-125 failed to show a significant increase in pSTAT3. Next, to confirm that let-7 and miR-125 did not bypass JAK-STAT signaling when added to *Dgcr8*$^{\Delta/\Delta}$ GPCs, we asked whether let-7 and miR-125 could rescue differentiation even in the absence of JAK-STAT signaling (Supplementary Fig S6). The introduction of JAKi to the differentiation media along with transfection of let-7 and miR-125 completely blocked the ability of the miRNAs to rescue GFAP

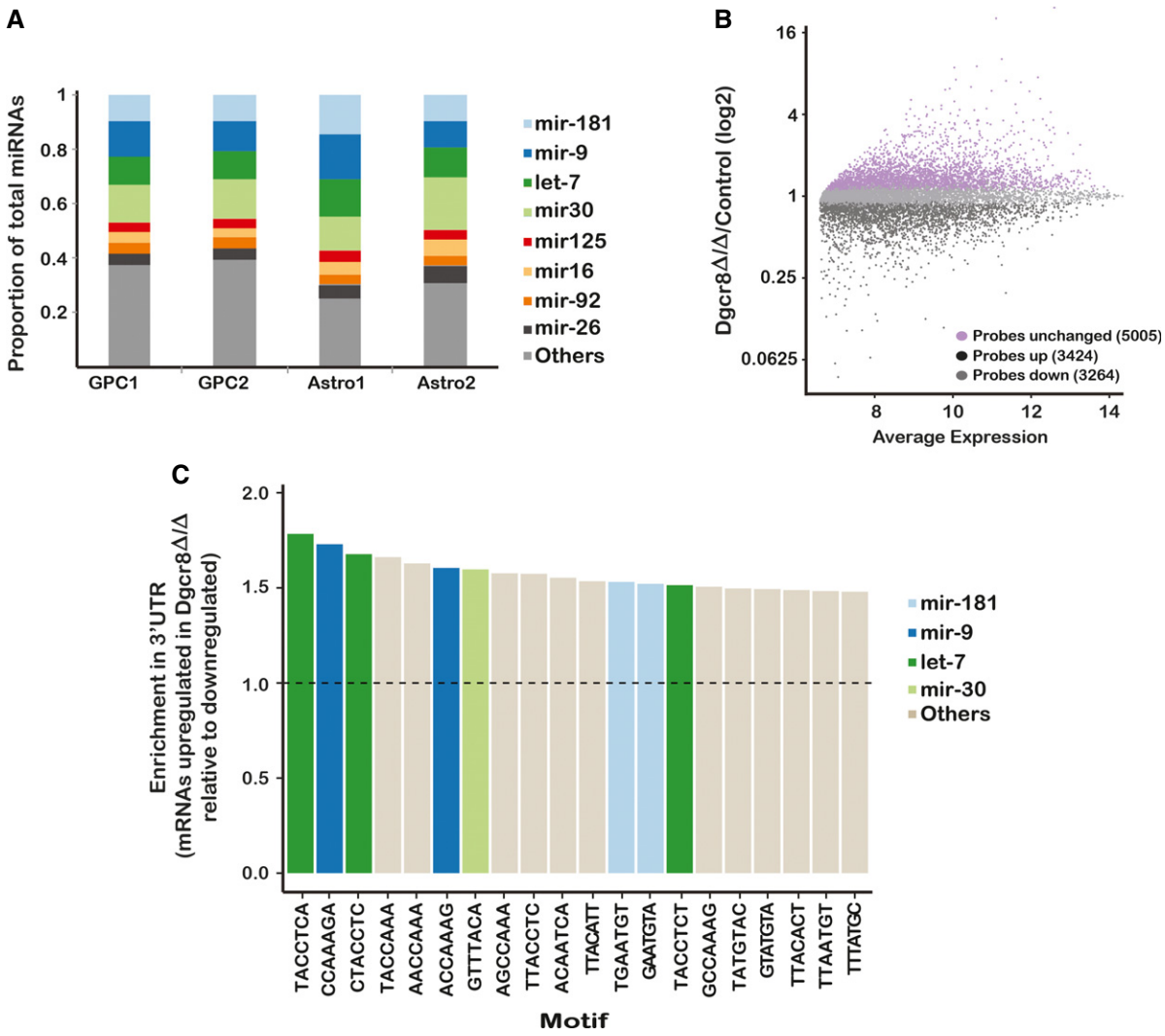

Figure 3. Loss of Dgcr8 leads to derepression of GPC miRNA targets.

A Distribution of miRNAs in GPCs and astrocytes from sequencing data.

B Microarray analysis of *Dgcr8*$^{\Delta/\Delta}$ GPCs relative to *Dgcr8*$^{flox/\Delta}$.

C Unbiased motif analysis of 3′ UTR of mRNAs upregulated in *Dgcr8*$^{\Delta/\Delta}$ GPCs and matches to miRNA seed sequences. Enrichment was calculated relative to mRNAs downregulated in *Dgcr8*$^{\Delta/\Delta}$ cells. A Fisher's exact test was performed and $P < 0.01$ cutoff was used to determine enriched motifs.

expression in *Dgcr8*$^{\Delta/\Delta}$ cells. These data suggest that there are two alternative means of rescuing *Dgcr8*$^{\Delta/\Delta}$ GPC differentiation: let-7/miR-125 introduction or activation of JAK-STAT by exogenous LIF. Therefore, the let-7/miR-125 miRNAs and JAK-STAT appear to act in parallel but interdependent pathways.

Next, we took the direct approach of identifying targets of let-7 and miR-125 in GPCs. While these two miRNAs have distinct seeds, they have been predicted to have a statistically significant overlap in targets, suggesting the ability of each of these miRNAs to rescue differentiation could be through the downregulation of a common set of mRNAs (Tsang *et al*, 2010). To identify direct and indirect targets of let-7 and miR-125 in GPCs, microarray analysis was performed on RNA isolated 24 h following transfection of *Dgcr8*$^{\Delta/\Delta}$ GPCs with let-7 and miR-125. Passage-matched mock-transfected *Dgcr8*$^{\Delta/\Delta}$ GPCs were used as control. As expected, hundreds of genes were up- and downregulated with an adjusted *P*-value cutoff of 0.01 (Fig 5A). To distinguish direct and indirect targets, the mRNAs were evaluated for sequences complementary to the seed sequence of the two miRNAs (Supplementary Fig S7A). There was a strong enrichment for the seed matches for both miRNAs within the open reading frame (ORF) and 3′ untranslated region (3′UTR) of downregulated genes (Fig 5B). In contrast, there was a depletion of seed matches in the upregulated genes. To further validate the target identification, we examined the levels of a number of known let-7 targets (Supplementary Fig S7B and C). A number of these genes that have previously been shown to be important in other contexts including pluripotency and earlier neural development (N-Myc, Hmga2, LIN28, Igf2bp1) were undetected in *Dgcr8*$^{\Delta/\Delta}$ GPCs (detection *P*-value < 0.5) (Supplementary Fig S7B) (Melton *et al*, 2010; Nishino *et al*, 2013; Patterson *et al*, 2014). However, other known targets identified as being part of a mid-gestation network of genes silenced by let-7 were expressed in GPCs, upregulated in *Dgcr8*$^{\Delta/\Delta}$

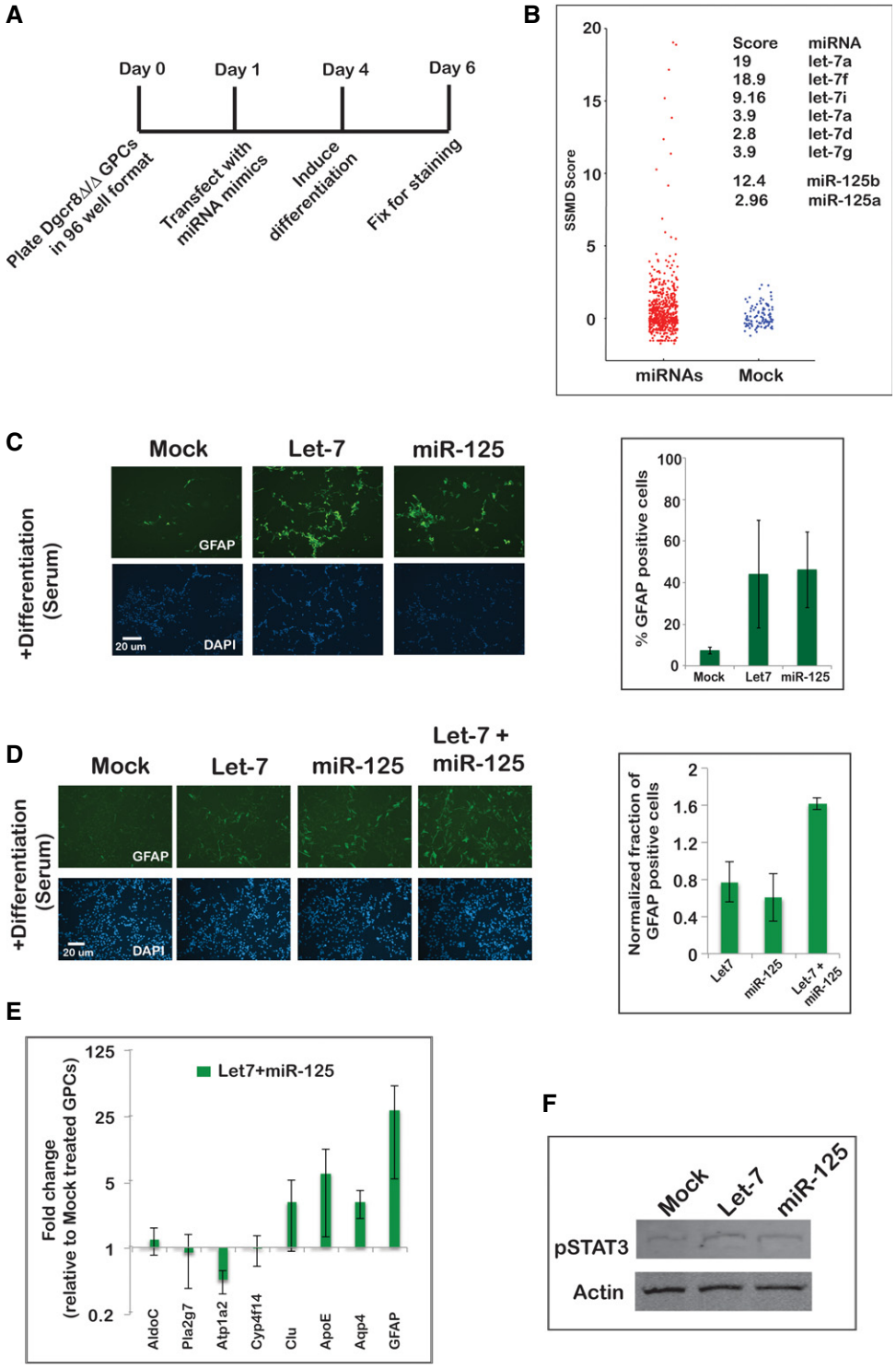

Figure 4. Let-7 and miR-125 miRNAs rescue astrocyte differentiation.

A Schematic of screen procedure.

B Results of miRNA screen in *Dgcr8*$^{\Delta/\Delta}$ GPCs. Each dot represents one well in the screen. Mock-treated wells were used as control and are shown in blue.

C Confirmation of let-7 and miR-125 screen hits with independently synthesized mimics. Quantification is shown on the right (n = 4).

D Synergistic rescue of GFAP expression by let-7 and miR-125. Total concentration of mimics in wells with miRNA was 50 nM (n = 3). Quantification of GFAP-positive cells in each well normalized to the mean of the experiment is shown on the right.

E RT–qPCR for panel of astrocyte markers in mock and let-7 + 125 treated *Dgcr8*$^{\Delta/\Delta}$ GPCs following 48 h of differentiation (n = 3).

F Representative blot of pSTAT3 levels 14 h post-differentiation following let-7 and miR-125 addition in *Dgcr8*$^{\Delta/\Delta}$ GPCs (n = 3).

Data information: In all panels, error bars represent SD. Scale bars as shown.

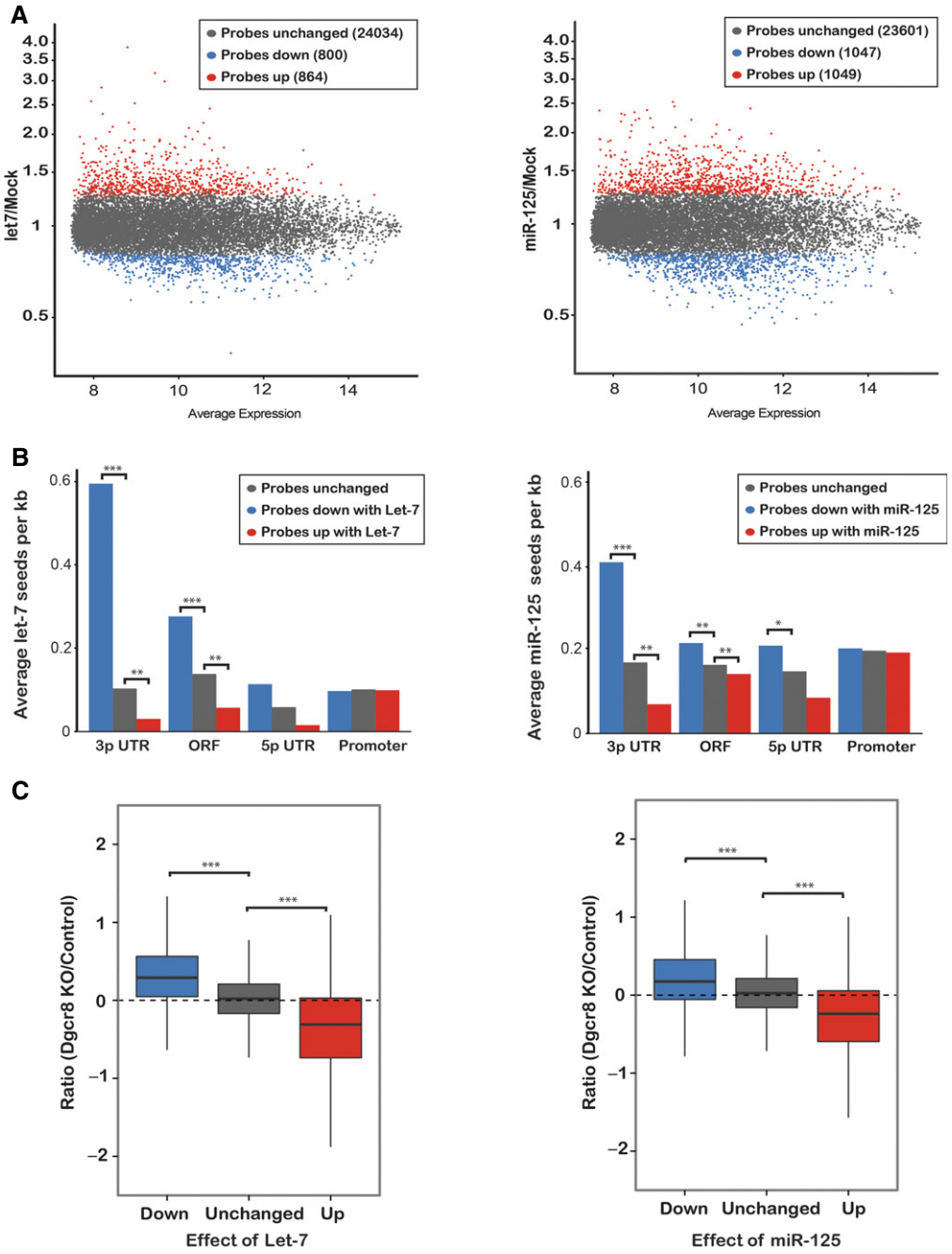

Figure 5. Let-7 and miR-125 suppress hundreds of transcripts by binding their 3′ UTR and ORFs.

A Microarray analysis following introduction of let-7 and miR-125 in *Dgcr8*$^{\Delta/\Delta}$ GPCs. Upregulated transcripts are shown in red, downregulated transcripts in blue (adjusted *P*-value < 0.05). Data shown is for average of 3 replicates.

B Analysis of seed matches in the promoter, 5′ UTR, ORF and 3′ UTR of downregulated and upregulated transcripts. Data are presented as the mean number of seeds matches per kb of sequence for the listed groups of altered genes described in (A). *P*-values calculated by the Wilcoxon rank-sum test and Bonferroni corrected are shown for $P < 0.01$ (***P-value < $1e^{-40}$, **P-value < $1.5e^{-8}$, *P-value < $1e^{-3}$).

C Box plots showing levels in *Dgcr8*$^{\Delta/\Delta}$ GPCs of probes upregulated, unchanged and downregulated upon addition of let-7 and miR-125. *P*-values were calculated using the Fisher's exact test (***represents $P < 2.2e^{-16}$).

cells and downregulated upon the addition of let-7 (Supplementary Fig S7C) (Gurtan *et al*, 2013). Therefore, the combination of downregulation upon miRNA introduction and seed matches in the 3′UTR/ORF uncovers a set of targets within the GPC context. Furthermore, many of the gene changes in the *Dgcr8*$^{\Delta/\Delta}$ GPCs could be reversed by simple addition of either let-7 or miR-125, consistent with these two miRNAs representing a large fraction of the miRNA pool in these cells (Figs 5C and 3A).

Due to the ability of let-7 and miR-125 to cooperate in rescuing differentiation in *Dgcr8*$^{\Delta/\Delta}$ cells, we sought to determine whether the mRNAs downregulated by the two miRNAs overlap greater than expected at random for expressed genes (Supplementary Fig S7D). Indeed, the overlap was highly significant suggesting that these miRNAs affect many common downstream genes and pathways.

To identify targets of let-7 and miR-125 whose upregulation might block GPC differentiation, we knocked down predicted targets in the *Dgcr8*$^{\Delta/\Delta}$ background and transferred cells to differentiation conditions. We selected candidate target genes by the following criteria: (i) downregulated with addition of let-7 and miR-125, (ii) contain a 3′UTR seed match for let-7 or 125, (iii) upregulated in *Dgcr8*$^{\Delta/\Delta}$ cells relative to control and (iv) unchanged or decreased during differentiation. This resulted in a list of 62 mRNAs (Supplementary Table S2). Cells were plated in 96-well format, and each well was transfected with an siRNA targeting each of the 62 mRNAs and placed in differentiation conditions the following day (Fig 6A). Surprisingly, in stark contrast to let-7 and miR-125, not a single siRNA pool to either the target set or a control set increased GFAP staining in *Dgcr8*$^{\Delta/\Delta}$ cells (Fig 6B). This finding suggests that either no single target can recapitulate the effects of the miRNAs or that the critical target did not fulfill the criteria for selection described above.

While knockdown of any one of these targets failed to rescue GFAP expression in *Dgcr8*$^{\Delta/\Delta}$ *cells*, it remained possible that the increased expression of any of these targets in knockout cells prevents normal differentiation of these cells. To test this hypothesis, we overexpressed candidate targets in wild-type GPCs and assessed differentiation capacity. From twenty-seven mRNAs co-targeted by both miRNAs (i.e., requiring predicted target sites for both miRNAs) (Supplementary Table S3), four were selected for overexpression. cDNAs encoding these proteins were cloned into expression constructs co-expressing mCherry. Luciferase was introduced as a negative control. Overexpression of two of the four targets, Plagl2 and Igf2bp2, robustly inhibited the number of GFAP-positive cells, while control, Ddx19b and Cbx2 overexpression did not affect differentiation (Fig 6C and Supplementary Fig S8A). These results combined with the results of individual target siRNA knockdown are consistent with a model where miRNAs target many mRNAs to block differentiation. However, we cannot exclude the possibility that a single untested target or combination of a small number of targets underlies the miRNA requirement.

mRNAs regulated by let-7 and miR-125 show consistent changes during *in vivo* astrocyte maturation

To assess the relevance of data from ESC-derived GPCs to *in vivo* astrocyte development, we overlapped let-7 and miR-125-regulated genes with profiling data of maturing astrocytes isolated from mouse spinal cords (Molofsky *et al*, 2013). Globally, mRNAs upregulated by addition of let-7 and miR-125 to *Dgcr8*$^{\Delta/\Delta}$ GPCs were upregulated during normal astrocyte maturation (Fig 6D and Supplementary Fig S8B). Conversely, mRNAs downregulated by let-7 and miR-125 were downregulated by addition of let-7 and miR-125 during astrocyte maturation. Together, these data support a role for let-7 and miR-125 modulating a molecular program consistent with astrocyte development *in vivo*.

It has been proposed that dedifferentiation of astrocytes via oncogene overexpression can lead to the formation of malignant gliomas (Friedmann-Morvinski *et al*, 2012). Since let-7 and miR-125 promote astrogliogenesis, we predicted that their targets may be misregulated in glioma, a tumor type associated with astrocyte dysfunction. Indeed, Plagl2 was previously identified as a negative regulator of astrocyte differentiation and is commonly amplified in glioma (Zheng *et al*, 2010a). To determine whether other mRNAs downregulated by let-7 and miR-125 in *Dgcr8*$^{\Delta/\Delta}$ cells are upregulated in gliomas, we overlapped let-7/miR-125-regulated genes with a previously identified 30-gene molecular signature of glioma stem cells (Sandberg *et al*, 2013) that is positively correlated with tumor severity. mRNAs downregulated by both miRNAs were strikingly enriched for the glioma stem cell molecular signature (Fig 6E). The highest enrichment was for mRNAs downregulated by both miRNAs, further providing support to the notion that let-7 and miR-125 co-target mRNAs inhibitory to astrocyte differentiation.

Discussion

Here, we have shown that Dgcr8 is essential for astrocyte differentiation *in vitro*, consistent with *in vivo* Dicer knockout-derived models (Andersson *et al*, 2010). Unlike past work, our *in vitro* system enabled discovery of specific miRNAs, pathways and targets that underlie major components of the differentiation defect. Let-7 and miR-125 rescued differentiation of *Dgcr8*$^{\Delta/\Delta}$ GPCs into cells with astrocyte-like morphology and expression of multiple mature astrocyte markers. Similarly, activation of the otherwise repressed JAK-STAT pathway was sufficient to rescue differentiation of the knockout GPCs to GFAP-positive cells. However, let-7 and miR-125 did not result in increased STAT3 phosphorylation placing these miRNAs in a parallel pathway to JAK-STAT signaling. The two miRNAs suppressed hundreds of targets in the GPCs, presumably priming them to respond to differentiation cues. Overexpression of a subset of individual targets in wild-type cells blocked astrocyte differentiation, but knockdown of any single candidate target in *Dgcr8*$^{\Delta/\Delta}$ cells was insufficient to recapitulate the effect of let-7 and miR-125. Therefore, let-7 and miR-125 appear to be functioning through numerous targets that otherwise cooperatively block differentiation. Interestingly, the genes directly and indirectly modulated by these miRNAs are similarly regulated during *in vivo* astrocyte maturation. Furthermore, mRNAs downregulated by let-7 and miR-125 are enriched for a gene signature correlated with glioma progression, a cancer associated with defects in astrocyte differentiation. Therefore, the *in vitro* findings presented here are clearly relevant to *in vivo* astrocyte differentiation, an area of research that has been relatively intractable due to the difficulty of isolating and manipulating GPCs within the organism.

This work provides insight into the role of specific miRNAs and their target genes in astrogliogenesis. The difficulty in isolating astrocyte progenitors *in vivo* has left a large gap in knowledge about astrocyte development, despite the dramatic rise in studies showing novel roles for astrocytes in CNS function and evolution (Han *et al*, 2013; Xie *et al*, 2013; Molofsky *et al*, 2014). Mechanisms underlying early astrocyte commitment of a gliogenic progenitor are largely unknown (Freeman, 2010). As miRNAs have evolved to target cooperative gene networks, it is possible to identify novel components of such networks by analyzing the targets of a given miRNA.

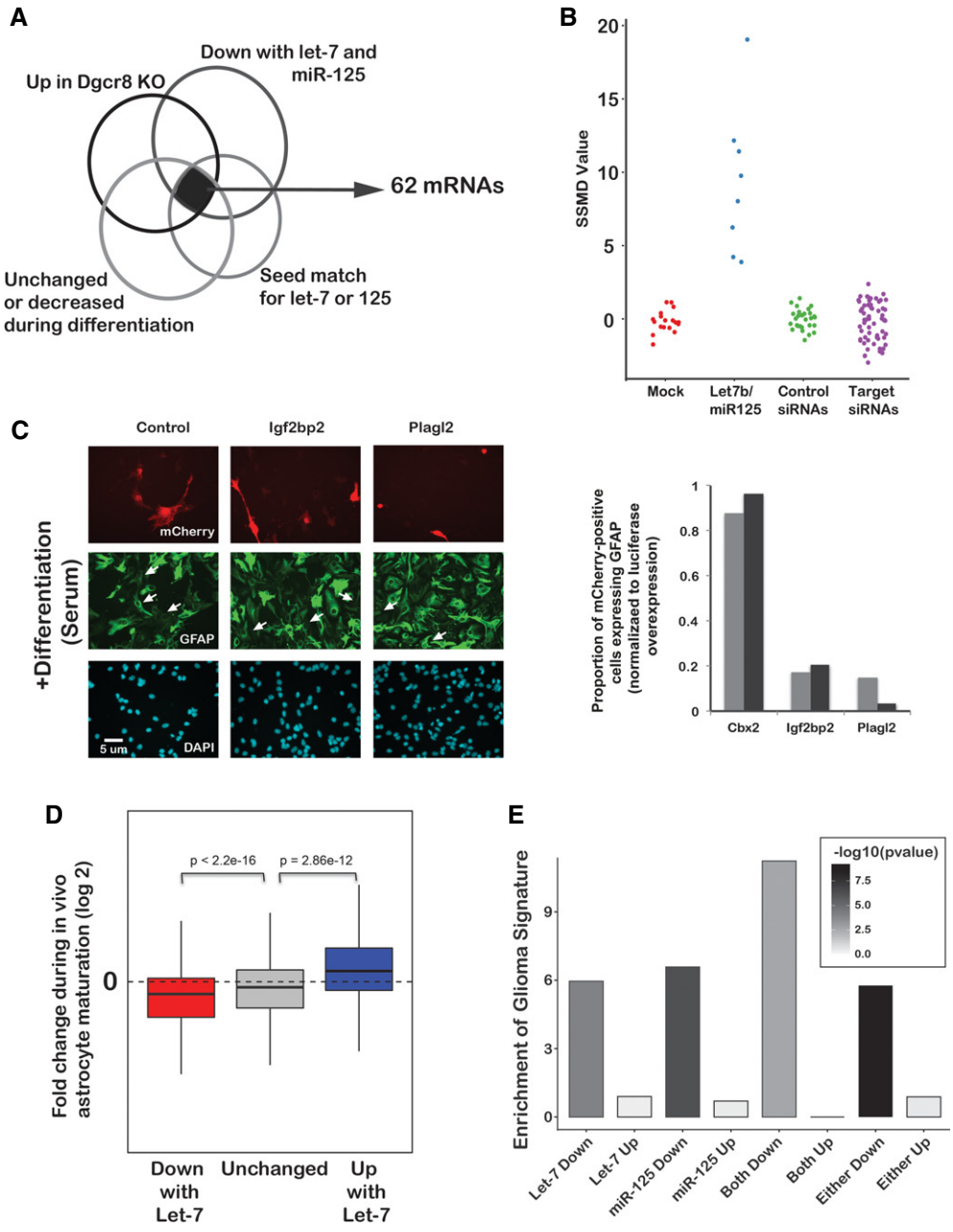

Figure 6. Targets of let-7 and miR-125 regulate astrocyte differentiation and are enriched in glioma stem cells.

A Schematic of criteria used for selecting functionally relevant targets.

B Results of siRNA screen of 62 targets of let-7/125 (n = 1). SSMD was calculated using control non-targeting siRNAs as negative reference. Let-7b and miR-125 were included as positive controls. Mock transfection and control siRNAs were used as negative controls.

C Constructs expressing mCherry along with the gene of interest (Cbx2, Plagl2, Igf2bp2) were nucleofected into GPCs. mCherry-positive cells were identified in each overexpression condition and their GFAP expression was scored (n = 2). Approximately 30–150 cells were counted in each overexpression experiment. Scale bar as shown. Light grey and dark grey bars represent the data for two experiments.

D Box plots showing levels of genes up- and downregulated following let-7 addition in *Dgcr8*$^{\Delta/\Delta}$ GPCs during astrocyte differentiation *in vivo*. *P*-values were calculated using Fisher's exact test.

E A glioma signature identified by Sandberg *et al* (2013) was overlapped with gene sets regulated by let-7 and miR-125 in *Dgcr8*$^{\Delta/\Delta}$ GPCs. Enrichment results are shown as a ratio of % of glioma genes in each group (as labeled on the *x*-axis) relative to % of glioma genes in the unchanged gene set.

In this study, we identify two miRNA families whose shared targets provide a rich candidate set of regulators of astrogliogenesis. Indeed, two out of four genes (Igf2bp2 and Plagl2) tested that are co-targeted by let-7 and miR-125 inhibit astrogliogenesis.

Previous studies in neural development have suggested diverse and age-dependent roles for let-7. Let-7 plays a role in promoting the switch between neurogenic and gliogenic potential of neural stem cells during fetal development by repressing Igf2bp1, Hmga2

and LIN28 (Nishino *et al*, 2013; Patterson *et al*, 2014). These mRNAs are lowly expressed in GPCs and not derepressed upon loss of Dgcr8. This suggests that during the neurogenic to gliogenic transition, increasing levels of let-7 may provide robustness to the regulatory mechanisms that lead to post-transcriptional silencing of these genes. As glial fate is specified and these targets are epigenetically silenced, let-7 targets gene networks inhibitory to terminal astrocyte differentiation. Consistent with let-7 targeting of the Igf2bp family members, two other family members of the Igf2bp family, Igf2bp2 and Igf2bp3, are actively repressed by let-7 and miR-125 in GPCs. In adult neural stem cells, one study has suggested that let-7 promotes both increased neurogenesis and gliogenesis via suppression of the stemness factor Tlx in neural stem cells (Zhao *et al*, 2010a). The fact that Tlx is lowly expressed and is unchanged with addition of let-7 in the context of Dgcr8 KO GPCs suggests context dependence of let-7 targets. Taken together, these studies suggest evolving roles for let-7 during gliogenesis.

Our study highlights how stem/progenitor cells utilize multiple, parallel and redundant pathways to ensure robust differentiation. First, characterizing shared targets of functionally overlapping miRNAs increases the likelihood of identifying a network of genes involved in a critical regulatory pathway. Let-7 and miR-125 are orthologs of let-7 and lin-4, heterochronic miRNAs in *Caenorhabditis elegans*. In *C. elegans*, these are among the small number of miRNAs that lead to a phenotype of delayed differentiation when deleted (Miska *et al*, 2007). While the two miRNAs are a bioinformatically predicted co-targeting pair, to date only a small number of common targets have been confirmed experimentally (Maller Schulman *et al*, 2008; La Torre *et al*, 2013). Two members of the families, let-7i and miR-125b, are co-transcribed, further suggesting a functional link. Here, we identify the largest set of mRNAs that are targeted by both miRNAs. As let-7 and miR-125 function through distinct seed sequences, this high degree of target overlap indicates that some evolutionary redundancy exists not only within miRNA families but also between miRNA families. Why such a large degree of redundancy exists remains to be determined. Further, as let-7 and miR-125 are broadly expressed, it remains to be determined whether this redundancy as well as their target gene networks is conserved across cell types.

We demonstrate that let-7 and miR-125 additionally share overlapping function with the JAK-STAT pathway canonically associated with astrogliogenesis. The activation of JAK-STAT or introduction of let-7/miR-125 could induce GFAP expression during differentiation of $Dgcr8^{\Delta/\Delta}$ GPCs. Multiple factors affect the transcriptional activity at the GFAP locus during differentiation, providing a means for multiple regulatory mechanisms to converge to ensure robust GFAP activation (Cheng *et al*, 2011). It will be interesting to determine in future studies how the JAK-STAT pathway and miRNAs converge to promote astrogliogenesis.

The dysfunction of astrocytes has been linked to the development of gliomas, including the malignant glioblastoma multiforme (GBM) (Friedmann-Morvinski *et al*, 2012). Indeed, the miRNAs and a number of targets that we identified as promoting astrogliogenesis are misregulated in gliomas. For example, Plagl2 is amplified in gliomas and inhibits differentiation of tumor-initiated cell lines (Zheng *et al*, 2010a). Additionally, in a number of cancers including gliomas, LIN28 has been identified as an oncogene, suggesting a misregulation of let-7 (Mao *et al*, 2013; Zhou *et al*, 2013; Qin *et al*, 2014). In cell lines derived from GBMs, overexpression of let-7 and miR-125 inhibits proliferation (Lee *et al*, 2010; Wu *et al*, 2012). The ability of these miRNAs to suppress proliferation in glioma cells may be in part associated with promoting differentiation.

In summary, the findings presented here demonstrate how two families of miRNAs can downregulate a common network of targets and cooperate with signaling pathways to prime a progenitor cell for differentiation. Importantly, these results provide a window into the molecular mechanisms that underlie the elusive GPC to astrocyte cell fate transition. Future work will need to bring together the multiple regulatory mechanisms driving this cell fate transition including signaling, transcriptional/epigenetic regulation, post-transcriptional and post-translation regulation. The *in vitro* GPC model provides an important entryway into these questions, which can then be further evaluated using *in vivo* models.

Materials and Methods

Cell culture and GPC derivation

ES cell culture has been previously described (Wang *et al*, 2007). Briefly, ES cells were maintained in media supplemented daily with 1,000 units/ml LIF. For neural differentiation, the protocol was adapted from a previously described method (Okabe *et al*, 1996; Brüstle & McKay, 1999). Briefly, ES cells were dissociated and grown as embryoid bodies (EBs) culture in media without LIF. EBs were plated in ITSF media as described by Okabe *et al* for 5–8 days and then dissociated into N2 media supplemented with 10 ng/ml FGF on to laminin-coated plates. Following 1–2 passages, 10 ng/ml EGF was added to the media along with FGF to stimulate glial specification. For differentiation, cells were grown to 70–80% confluency unless described otherwise. Growth factors were withdrawn, and N2 media supplemented with 1% FBS and B27 was added for 24–48 h.

To induce Dgcr8 loss, GPCs were treated with 1 μM tamoxifen for 16–24 h and, 2 days later, treated with 200 nM tamoxifen for 16–24 h to stimulate efficient Cre-lox-mediated recombination. To minimize cell death following loss of Dgcr8, cells were supplemented daily with growth factors until inducing differentiation.

For experiments with inhibitors, JAKi (AG490; Tocris Biosciences) was resuspended in DMSO and used at a final concentration of 1 μM. LIF was used at a concentration of 2,500–5,000 units/ml of media.

miRNA screen

A library of 570 miRNA mimics described previously was transfected into Dgcr8 KO GPCs plated in 96-well format in proliferation conditions (+EGF/FGF) (Wang *et al*, 2008). All mimics were transfected at a final concentration of 50 nM using DharmaFECT3. Differentiation was induced 3 days post-transfection with low serum addition and growth factor withdrawal. Following 48 h in differentiation conditions, plates were fixed and processed for GFAP immunofluorescence (anti-GFAP; Dako Cytomation Z0334). A DAPI counterstain was performed. All plates were imaged at 10× magnification using a high-throughput high-content fluorescent microscope system (InCell Analyzer, GE). The InCell Workstation software was used for analysis using the multitarget analysis module to count

number of total cells (DAPI) and percent of GFAP$^+$ cells. Hits identified by this system were then validated by eye. Significance of change in GFAP staining was calculated using strictly standardized mean difference (SSMD) score. Criteria for positive hits chosen for follow-up studies were (i) SSMD score > 2.5, (ii) rescue by multiple members of a miRNA family and (iii) expressed in GPCs or astrocytes.

Flow cytometry

Cells were passaged for flow cytometry and resuspended at a concentration of 150,000 cells/500 μl in Annexin-binding buffer. Annexin-APC (Invitrogen A35110, 1:500) and Sytox Blue (1:1,000) were added. Cells were analyzed on a BD LSRII instrument. Cells double-positive for Annexin and Sytox Blue were scored as apoptotic.

Transfections

miRNA mimics were ordered from Dharmacon, resuspended in sterile H_2O and transfected using the DharmaFECT3 reagent at a final concentration of 50–100 nM. Media was changed 24 h later and differentiation was induced 72 h following transfection. For the miRNA target knockdown screen, Dharmacon siGenome smartpool siRNAs were used at a final concentration of 50 nM.

Animal use

All animal experiments described here were approved by the Institutional Animal Care and Use Committee (IACUC) of the University of California, San Francisco.

Plasmid overexpression

For overexpression of miRNA target genes, cDNAs were cloned into a vector driven by EF1alpha and contained a T2A-mCherry element downstream of the cloned insert. Nucleofection was performed using the Glial cell kit with the 'A033' program to express the plasmid in GPCs. Differentiation was induced 24 h following nucleofection and cells were fixed 30–40 h later and processed for immunofluorescence.

Immunofluorescence

For immunofluorescence, cells were fixed in 4% PFA for 10–15 min, permeabilized with PBS containing 0.2% Triton-X100 and blocked in PBS containing 2% BSA and 1% goat serum. Primary and secondary antibody incubation was done in blocking solution, and cells were counterstained with DAPI. Secondary antibodies (Alexa Fluor) were used at a dilution of 1:500. Rat mCherry antibody was used at a dilution of 1:500 (Clontech).

Microarray analysis

RNA for all microarray samples was extracted from cells following lysis with Trizol (Invitrogen) and processed for Illumina bead chip arrays at the UCLA genome core facility. Microarrays of control and *Dgcr8* knockout GPCs (mock transfected) were performed 7 days following tamoxifen treatment. Quantile normalization was performed using the R/Bioconductor package beadarray, and differential expression analysis was performed using the R package Limma (Dunning *et al*, 2007). For discovery of let-7 and miR-125 targets, microarrays were performed 24 h post-transfection with let-7 and miR-125. Arrays were quantile normalized using the beadarray package. As one pair of mock and let-7 arrays was performed at a separate time, differential expression analysis was performed using the RankProd R package. Seed enrichment analysis was performed as previously described using custom python scripts and R code (Melton *et al*, 2010).

For analysis of Affymetrix data from Molofsky *et al*, microarrays were first normalized by RMA method using the 'Affy' R package. The fold change between e13 and e18 embryonic day astrocyte samples was used for further analysis. Triplicate array experiments were averaged. To overlap *in vitro* (Illumina) and the *in vivo* (Affymetrix) data, all probes that crossed a detection *P*-value of 0.05 in the Illumina array were overlapped by gene name in the Affymetrix array. For multiple probes with the same gene name, probes exhibiting the highest change were used.

Motif analysis was performed by matching and extracting 3p-UTR sequences from mm9 RefSeq mRNA transcripts for each Illumina probe ID. Redundant probes were removed so that no two probes mapped to a shared RefSeq transcript. For probes matching to multiple transcripts, the matched UTR with the largest length was retained. Transcripts were divided into experimental and control groups, and within each group, all UTRs were scanned and counts of every observed 7-mer motif were generated. For each unique 7-mer motif, the probability of observing k or more counts in the experiment was determined using Fisher's exact test.

RT-qPCR

RNA for all qPCR experiments was extracted using Trizol and quantified using a nanodrop spectrophotometer. One microgram of RNA was DNase-treated and reverse-transcribed using random hexamer primers and the Superscript III first strand synthesis kit (Invitrogen). qPCRs were performed on an ABI 7900 system. RT–qPCR primer sequences are listed below.

Cyp4f14, Forward	ctcttggtgagtgctggtga
Cyp4f14, Reverse	gcatgatgttggtgctatcg
AldoC, Forward	ggggtcatcttcttccatga
AldoC, Reverse	acccttgtcaaccttgatgc
Pla2g7, Forward	gtgcaccagaactttgacga
Pla2g7, Reverse	gctttgttggtgaggtcgat
Atp1a2, Forward	attgtgattgccacaggtga
Atp1a2, Reverse	ctccatggctatgggtgtct
Aqp4, Forward	acatggaggtggaggacaac
Aqp4, Reverse	ttctccacggtcaatgtcaa

Western blots

For protein extraction, cells were lysed in first lysed in weak lysis buffer (low NP40 lysis buffer—12.5 mM Tris pH 7.5, or 7.9/

150 mM NaCl, 100 μM EDTA, 10% glycerol, 0.1% NP-40) containing protease inhibitors (Roche) and phosphatase inhibitors (PhosphSTOP; Roche), followed by 3 freeze–thaw cycles in liquid nitrogen. The supernatant was collected following a high speed spin at 12,000 *g* and used for Western blots. Proteins were quantified using a Bradford assay with BSA standards. Approximately 20–25 μg of protein was used per lane. Antibodies were used at the following concentrations: pSTAT3 (Cell Signaling # 9145)—1:1,000, total STAT3 (Cell Signaling #9139), pSMAD1/5/8 (Cell Signaling #9511) and actin (Sigma, A4700). Primary antibody incubation was performed at room temperature for 2 h or overnight at 4°C. Secondary antibodies (Thermofisher) were used at a concentration of 1:10,000. Imaging was performed using an Odyssey LICOR scanner. Quantification was performed using ImageJ software.

An initial Western blot for pSTAT3 in $Dgcr8^{f/\Delta}$ cells showed levels increase significantly with a latency of > 1 h and are apparent at 5 h following the addition of BMP-4 (data not shown). Thus, a time point of 5 h or later was used for all subsequent experiments to ensure observable activation.

Small RNA sequencing and analysis

Total RNA was extracted using Trizol Reagent (Invitrogen). Small RNAs were cloned and multiplexed using the Illumina Tru-Seq kit protocol and in house reagents. 3′ adapter was adenylated prior to small RNA cloning as described previously (Babiarz *et al*, 2008). All adapters and PCR primers were purified on a 22% urea-acrylamide gel prior to use. Libraries were diluted to 10 nM and sequenced on a HiSeq 2000 at UCSF.

Small RNA sequencing data were processed using custom perl scripts and mapped to miRNAs using Bowtie (-p4 -f -v0 -k5 -m5 options) (Langmead *et al*, 2009). Sequences were trimmed of the 3′ adapter by requiring 8 nt of perfect match to the adapter sequence. Sequences were mapped to the mouse pre-miRNA hairpins in miRBase v20.0. All reads perfectly mapping no more than to five hairpins were included in counts. Reads mapping to multiple miRNAs were divided by the number of mappings and then assigned to individual miRNAs. Read counts for each miRNA seed family were summarized and reported as a percentage of total miRNA reads. Targetscan miRNA families were used to group miRNAs into seed families.

Accession numbers

All microarray data and small RNA sequencing data have been submitted to the GEO repository. Microarray data are available under Accession Number GSE64637 and small RNA sequencing data under GSE64661.

Supplementary information for this article is available online: http://emboj.embopress.org

Acknowledgements

We would like to thank members of the Blelloch laboratory, especially Amy Chen, Jake Freimer, Raga Krishnakumar, Ronald Parchem, Mayya Shveygert and John Vincent for critical reading of the manuscript. We would like to thank Collin Melton for assistance with statistics and bioinformatic analysis, and Nicole Moore, Jason Liu and Glencijoy David for technical assistance. We would like to thank Luis C Fuentealba (Alvarez-Buylla laboratory) for training and advice on transplantation experiments. We would like to thank Justin Ellis (Rowitch laboratory) for brain sections and antibodies. We would like to thank Fong Ming Koh (Ramalho-Santos lab) for overexpression constructs. This work was funded by a CIRM training grant TG2-01153 (A.S.) and grants to R.H.B. from the US National Institutes of Health (NINDS R01 NS057221 and NIGMS R01 GM101180) and the California Institute of Regenerative Medicine (New Faculty Award, RN2-00906-1).

Author contributions

RHB and AS conceived the project, designed experiments and wrote the manuscript. AS contributed to experiments in all figures. MD contributed to experiments in Figs 1 and 2 and Supplementary Figs S2 and S3.

Conflict of interest

The authors declare that they have no conflict of interest.

References

Andersson T, Rahman S, Sansom SN, Alsiö JM, Kaneda M, Smith J, O'Carroll D, Tarakhovsky A, Livesey FJ (2010) Reversible block of mouse neural stem cell differentiation in the absence of dicer and microRNAs. *PLoS One* 5: e13453

Babiarz JE, Ruby JG, Wang Y, Bartel DP, Blelloch R (2008) Mouse ES cells express endogenous shRNAs, siRNAs, and other Microprocessor-independent, Dicer-dependent small RNAs. *Genes Dev* 22: 2773–2785

Barad O, Mann M, Chapnik E, Shenoy A, Blelloch R, Barkai N, Hornstein E (2012) Efficiency and specificity in microRNA biogenesis. *Nat Struct Mol Biol* 19: 650–652

Bonni A, Sun Y, Nadal-Vicens M, Bhatt A, Frank DA (1997) Regulation of gliogenesis in the central nervous system by the JAK-STAT signaling pathway. *Science* 278: 477–483

Brüstle O, McKay RDG (1999) Embryonic stem cell-derived glial precursors: a source of myelinating transplants. *Science* 285: 754–756

Cahoy JD, Emery B, Kaushal A, Foo LC, Zamanian JL, Christopherson KS, Xing Y, Lubischer JL, Krieg PA, Krupenko SA, Thompson WJ, Barres BA (2008) A transcriptome database for astrocytes, neurons, and oligodendrocytes: a new resource for understanding brain development and function. *J Neurosci* 28: 264–278

Cheng P-Y, Lin Y-P, Chen Y-L, Lee Y-C, Tai C-C, Wang Y-T, Chen Y-J, Kao C-F, Yu J (2011) Interplay between SIN3A and STAT3 mediates chromatin conformational changes and GFAP expression during cellular differentiation. *PLoS One* 6: e22018

Dugas JC, Cuellar TL, Scholze A, Ason B, Ibrahim A, Emery B, Zamanian JL, Foo LC, McManus MT, Barres BA (2010) Dicer1 and miR-219 Are required for normal oligodendrocyte differentiation and myelination. *Neuron* 65: 597–611

Dunning MJ, Smith ML, Ritchie ME, Tavaré S (2007) beadarray: r classes and methods for Illumina bead-based data. *Bioinformatics* 23: 2183–2184

Fan G, Martinowich K, Chin MH, He F, Fouse SD, Hutnick L, Hattori D, Ge W, Shen Y, Wu H, ten Hoeve J, Shuai K, Sun YE (2005) DNA methylation controls the timing of astrogliogenesis through regulation of JAK-STAT signaling. *Development* 132: 3345–3356

Freeman MR (2010) Specification and morphogenesis of astrocytes. *Science* 330: 774–778

Friedmann-Morvinski D, Bushong EA, Ke E, Soda Y, Marumoto T, Singer O, Ellisman MH, Verma IM (2012) Dedifferentiation of neurons and astrocytes by oncogenes can induce gliomas in mice. *Science* 338: 1080 – 1084

Fukuda S, Abematsu M, Mori H, Yanagisawa M, Kagawa T, Nakashima K, Yoshimura A, Taga T (2007) Potentiation of astrogliogenesis by STAT3-mediated activation of bone morphogenetic protein-Smad signaling in neural stem cells. *Mol Cell Biol* 27: 4931 – 4937

Giraldez AJ, Cinalli RM, Glasner ME, Enright AJ, Thomson JM, Baskerville S, Hammond SM, Bartel DP, Schier AF (2005) MicroRNAs regulate brain morphogenesis in zebrafish. *Science* 308: 833 – 838

Goljanek-Whysall K, Sweetman D, Abu-Elmagd M, Chapnik E, Dalmay T, Hornstein E, Münsterberg A (2011) MicroRNA regulation of the paired-box transcription factor Pax3 confers robustness to developmental timing of myogenesis. *Proc Natl Acad Sci USA* 108: 11936 – 11941

Gurtan AM, Ravi A, Rahl PB, Bosson AD, JnBaptiste CK, Bhutkar A, Whittaker CA, Young RA, Sharp PA (2013) Let-7 represses Nr6a1 and a mid-gestation developmental program in adult fibroblasts. *Genes Dev* 27: 941 – 954

Han X, Chen M, Wang F, Windrem M, Wang S, Shanz S, Xu Q, Oberheim NA, Bekar L, Betstadt S, Silva AJ, Takano T, Goldman SA, Nedergaard M (2013) Forebrain engraftment by human glial progenitors enhances synaptic plasticity and learning in adult mice. *Cell Stem Cell* 12: 342 – 353

He F, Ge W, Martinowich K, Becker-Catania S, Coskun V, Zhu W, Wu H, Castro D, Guillemot F, Fan G, de Vellis J, Sun YE (2005) A positive autoregulatory loop of Jak-STAT signaling controls the onset of astrogliogenesis. *Nat Neurosci* 8: 616 – 625

Judson RL, Greve TS, Parchem RJ, Blelloch R (2013) MicroRNA-based discovery of barriers to dedifferentiation of fibroblasts to pluripotent stem cells. *Nat Struct Mol Biol* 20: 1227 – 1235

Krencik R, Weick JP, Liu Y, Zhang Z-J, Zhang S-C (2011) Specification of transplantable astroglial subtypes from human pluripotent stem cells. *Nat Biotechnol* 29: 528 – 534

Krichevsky AM, Sonntag K-C, Isacson O, Kosik KS (2009) Specific microRNAs modulate embryonic stem cell-derived neurogenesis. *Stem Cells* 24: 857 – 864

Krol J, Loedige I, Filipowicz W (2010) The widespread regulation of microRNA biogenesis, function and decay. *Nat Rev Genet* 11: 597 – 610

La Torre A, Georgi S, Reh TA (2013) Conserved microRNA pathway regulates developmental timing of retinal neurogenesis. *Proc Natl Acad Sci USA* 110: E2362 – E2370

Langmead B, Trapnell C, Pop M, Salzberg SL (2009) Ultrafast and memory-efficient alignment of short DNA sequences to the human genome. *Genome Biol* 10: R25

Lee S-T, Chu K, Oh H-J, Im W-S, Lim J-Y, Kim S-K, Park C-K, Jung K-H, Lee SK, Kim M, Roh J-K (2010) Let-7 microRNA inhibits the proliferation of human glioblastoma cells. *J Neurooncol* 102: 19 – 24

Lindsten T, Golden JA, Zong W-X, Minarcik J, Harris MH, Thompson CB (2003) The proapoptotic activities of bax and bak limit the size of the neural stem cell pool. *J Neurosci* 23: 11112 – 11119

Lovatt D, Sonnewald U, Waagepetersen HS, Schousboe A, He W, Lin JH-C, Han X, Takano T, Wang S, Sim FJ, Goldman SA, Nedergaard M (2007) The transcriptome and metabolic gene signature of protoplasmic astrocytes in the adult murine cortex. *J Neurosci* 27: 12255 – 12266

Maller Schulman BR, Liang X, Stahlhut C, DelConte C, Stefani G, Slack FJ (2008) The let-7 microRNA target gene, Mlin41/Trim71 is required for mouse embryonic survival and neural tube closure. *Cell Cycle* 7: 3935 – 3942

Mao X-G, Hütt-Cabezas M, Orr BA, Weingart M, Taylor I, Rajan AKD, Odia Y, Kahlert U, Maciaczyk J, Nikkhah G, Eberhart CG, Raabe EH (2013) LIN28A facilitates the transformation of human neural stem cells and promotes glioblastoma tumorigenesis through a pro-invasive genetic program. *Oncotarget* 4: 1050 – 1064

Melton C, Judson RL, Blelloch R (2010) Opposing microRNA families regulate self-renewal in mouse embryonic stem cells. *Nature* 463: 621 – 626

Miska EA, Alvarez-Saavedra E, Abbott AL, Lau NC, Hellman AB, McGonagle SM, Bartel DP, Ambros VR, Horvitz HR (2007) Most *Caenorhabditis elegans* microRNAs are individually not essential for development or viability. *PLoS Genet* 3: e215

Molofsky AV, Krencik R, Krenick R, Ullian EM, Ullian E, Tsai H-H, Deneen B, Richardson WD, Barres BA, Rowitch DH (2012) Astrocytes and disease: a neurodevelopmental perspective. *Genes Dev* 26: 891 – 907

Molofsky AV, Glasgow SM, Chaboub LS, Tsai H-H, Murnen AT, Kelley KW, Fancy SPJ, Yuen TJ, Madireddy L, Baranzini S, Deneen B, Rowitch DH, Oldham MC (2013) Expression profiling of Aldh1 l1-precursors in the developing spinal cord reveals glial lineage-specific genes and direct Sox9-Nfe2 l1 interactions. *Glia* 61: 1518 – 1532

Molofsky AV, Kelley KW, Tsai H-H, Redmond SA, Chang SM, Madireddy L, Chan JR, Baranzini SE, Ullian EM, Rowitch DH (2014) Astrocyte-encoded positional cues maintain sensorimotor circuit integrity. *Nature* 509: 189 – 194

Nicholas CR, Chen J, Tang Y, Southwell DG, Chalmers N, Vogt D, Arnold CM, Chen Y-JJ, Stanley EG, Elefanty AG, Sasai Y, Alvarez-Buylla A, Rubenstein JLR, Kriegstein AR (2013) Functional maturation of hPSC-derived forebrain interneurons requires an extended timeline and mimics human neural development. *Cell Stem Cell* 12: 573 – 586

Nishino J, Kim S, Zhu Y, Zhu H, Morrison SJ, Rossant J (2013) A network of heterochronic genes including Imp1 regulates temporal changes in stem cell properties. *eLife* 2: e00924 – e00924

Okabe S, Forsberg-Nilsson K, Spiro AC, Segal M, McKay RDG (1996) Development of neuronal precursor cells and functional postmitotic neurons from embryonic stem cells in vitro. *Mech Dev* 59: 89 – 102

Patterson M, Gaeta X, Loo K, Edwards M, Smale S, Cinkornpumin J, Xie Y, Listgarten J, Azghadi S, Douglass SM, Pellegrini M, Lowry WE (2014) let-7 miRNAs can act through notch to regulate human gliogenesis. *Stem Cell Rep* 3: 758 – 773

Preiss T ed. (2009) Genomic analysis suggests that mRNA destabilization by the microprocessor is specialized for the auto-regulation of Dgcr8. *PLoS One* 4: e6971 – e6971

Qin R, Zhou J, Chen C, Xu T, Yan Y, Ma Y, Zheng Z, Shen Y, Lu Y, Fu D, Chen J (2014) LIN28 is involved in glioma carcinogenesis and predicts outcomes of glioblastoma multiforme patients. *PLoS One* 9: e86446

Rowitch DH, Kriegstein AR (2010) Developmental genetics of vertebrate glial-cell specification. *Nature* 468: 214 – 222

Sandberg CJ, Altschuler G, Jeong J, Strømme KK, Stangeland B, Murrell W, Grasmo-Wendler U-H, Myklebost O, Helseth E, Vik-Mo EO, Hide W, Langmoen IA (2013) Comparison of glioma stem cells to neural stem cells from the adult human brain identifies dysregulated Wnt-signaling and a fingerprint associated with clinical outcome. *Exp Cell Res* 319: 2230 – 2243

Seong Y, Lim D-H, Kim A, Seo JH, Lee YS, Song H, Kwon Y-S (2014) Global identification of target recognition and cleavage by the Microprocessor in human ES cells. *Nucleic Acids Res* 42: 12806 – 12821

Sinkkonen L, Hugenschmidt T, Berninger P, Gaidatzis D, Mohn F, Artus-Revel CG, Zavolan M, Svoboda P, Filipowicz W (2008) MicroRNAs control de

novo DNA methylation through regulation of transcriptional repressors in mouse embryonic stem cells. *Nat Struct Mol Biol* 15: 259 – 267

Steiner DF, Thomas MF, Hu JK, Yang Z, Babiarz JE, Allen CDC, Matloubian M, Blelloch R, Ansel KM (2011) MicroRNA-29 regulates T-box transcription factors and interferon-γ production in helper T cells. *Immunity* 35: 169 – 181

Tsang JS, Ebert MS, van Oudenaarden A (2010) Genome-wide dissection of microRNA functions and cotargeting networks using gene set signatures. *Mol Cell* 38: 140 – 153

Wang Y, Medvid R, Melton C, Jaenisch R, Blelloch R (2007) DGCR8 is essential for microRNA biogenesis and silencing of embryonic stem cell self-renewal. *Nat Genet* 39: 380 – 385

Wang Y, Baskerville S, Shenoy A, Babiarz JE, Baehner L, Blelloch R (2008) Embryonic stem cell-specific microRNAs regulate the G1-S transition and promote rapid proliferation. *Nat Genet* 40: 1478 – 1483

Wang Y, Melton C, Li Y-P, Shenoy A, Zhang X-X, Subramanyam D, Blelloch R (2013) miR-294/miR-302 promotes proliferation, suppresses G1-S restriction point, and inhibits ESC differentiation through separable mechanisms. *Cell Rep* 4: 99 – 109

Wu N, Xiao L, Zhao X, Zhao J, Wang J, Wang F, Cao S, Lin X (2012) miR-125b regulates the proliferation of glioblastoma stem cells by targeting E2F2. *FEBS Lett* 586: 3831 – 3839

Xie L, Kang H, Xu Q, Chen MJ, Liao Y, Thiyagarajan M, O'Donnell J, Christensen DJ, Nicholson C, Iliff JJ, Takano T, Deane R, Nedergaard M (2013) Sleep drives metabolite clearance from the adult brain. *Science* 342: 373 – 377

Yi R, Pasolli HA, Landthaler M, Hafner M, Ojo T, Sheridan R, Sander C, O'Carroll D, Stoffel M, Tuschl T, Fuchs E (2009) DGCR8-dependent microRNA biogenesis is essential for skin development. *Proc Natl Acad Sci USA* 106: 498 – 502

Yoo AS, Staahl BT, Chen L, Crabtree GR (2009) MicroRNA-mediated switching of chromatin-remodelling complexes in neural development. *Nature* 460: 642 – 646

Zhang Y, Barres BA (2010) Astrocyte heterogeneity: an underappreciated topic in neurobiology. *Curr Opin Neurobiol* 20: 588 – 594

Zhao C, Sun G, Li S, Shi Y (2009) A feedback regulatory loop involving microRNA-9 and nuclear receptor TLX in neural stem cell fate determination. *Nat Struct Mol Biol* 16: 365 – 371

Zhao C, Sun G, Li S, Lang MF, Yang S, Li W, Shi Y (2010a) MicroRNA let-7b regulates neural stem cell proliferation and differentiation by targeting nuclear receptor TLX signaling. *Proc Natl Acad Sci USA* 107: 1876 – 1881

Zhao X, He X, Han X, Yu Y, Ye F, Chen Y, Hoang T, Xu X, Mi Q-S, Xin M (2010b) MicroRNA-mediated control of oligodendrocyte differentiation. *Neuron* 65: 612 – 626

Zheng H, Ying H, Wiedemeyer R, Yan H, Quayle SN, Ivanova EV, Paik J-H, Zhang H, Xiao Y, Perry SR, Hu J, Vinjamoori A, Gan B, Sahin E, Chheda MG, Brennan C, Wang YA, Hahn WC, Chin L, DePinho RA (2010a) PLAGL2 regulates Wnt signaling to impede differentiation in neural stem cells and gliomas. *Cancer Cell* 17: 497 – 509

Zheng K, Li H, Zhu Y, Zhu Q, Qiu M (2010b) MicroRNAs are essential for the developmental switch from neurogenesis to gliogenesis in the developing spinal cord. *J Neurosci* 30: 8245 – 8250

Zhou J, Ng S-B, Chng W-J (2013) LIN28/LIN28B: an emerging oncogenic driver in cancer stem cells. *Int J Biochem Cell Biol* 45: 973 – 978

